

## Photochemical Degradation of Poly(ethylene Terephthalate). III. Determination of Decomposition Products and Reaction Mechanism

M. DAY\* and D. M. WILES, *Division of Chemistry,  
National Research Council of Canada, Ottawa 7, Canada*

### Synopsis

The vacuum photolysis and air photo-oxidation of poly(ethylene terephthalate) were studied using light in the wavelength ranges of 225–420 nm and 300–420 nm. The volatile photodegradation products were determined by mass-spectrometric and gas-chromatographic analysis; CO and CO<sub>2</sub> were found to be the predominant products. In addition, the rates of formation of carboxylic acid endgroups and the net weight losses of the film samples were determined as a function of irradiation time. Quantum yields for the initial rates of formation of CO and CO<sub>2</sub> and of —COOH within the film were calculated. On the basis of the results obtained, in this and the preceding papers in this series, reaction mechanisms have been proposed for the photochemical degradation of the polymer. The production of CO and —COOH in both vacuum and air have been attributed mainly to a Norrish type I cleavage and a Norrish type II photorearrangement, respectively. It has also been concluded that, in the presence of air, an oxidative reaction sequence occurs whereby alkyl radicals produced on photolysis react with oxygen to form ROO· radicals. These subsequently react further to produce CO<sub>2</sub> as the main volatile product of photo-oxidation.

### INTRODUCTION

Exposure of poly(ethylene terephthalate) (PET) to terrestrial sunlight and certain artificial light sources causes a deterioration in the physical properties of the polymer, such as loss in strength and elasticity. This deterioration is accompanied by a reduction in the molecular weight of the polymer and changes in the chemical composition.

We have already reported in part I<sup>1</sup> the changes which occur in some physical and chemical properties of PET on exposure to ultraviolet (UV) light. In part II,<sup>2</sup> the importance of wavelength of irradiation and environment on the decomposition was considered. The work described in this paper is concerned with the determination of the volatile decomposition products and the calculation of quantum yields for the initial photochemical reactions. Although the photodegradation of PET has been studied by several workers (see ref. 2 and the references quoted therein), few attempts have been made to study the chemical changes occurring in order to satis-

\* NRCC Postdoctoral Fellow 1969–1971.

factorily explain all the known aspects of the photochemical decomposition.

From a practical point of view, the main interest lies in the degradation occurring in the presence of air; however, studies were also made of the vacuum photolysis of PET. Thus, by investigating the chemical consequences of vacuum photolysis and of photo-oxidation individually, it should be possible to determine the fundamental chemical reactions occurring in the photochemical decomposition of PET.

### EXPERIMENTAL

The PET film (du Pont Mylar) was 21  $\mu$  thick with a density of 1.398, corresponding to a crystallinity of approximately 50%.<sup>3</sup> The viscosity-average molecular weight of the film was calculated to be 19,700 from the expression of Ravens<sup>4</sup> using *o*-chlorophenol at 25°C. The oligomeric content was estimated, according to the method of Peebles et al.,<sup>5</sup> to be 2.8 wt-% on the basis of a 14-day Soxhlet extraction with xylene. TLC analysis of this low molecular weight material indicated that the cyclic trimer was the predominant species, with smaller amounts of the cyclic tetramer and cyclic pentamer also present.

Irradiations were performed in quartz cells in an atmosphere of air or under vacuum. The lamp used was an Osram superpressure mercury lamp (SP 500 W). The light from the lamp was focused into a parallel beam by quartz lenses and filtered through a 10-cm-path water filter. Corning glass filters were used to select the two working wavelength regions chosen for these studies. The wavelength region of 225–420 nm (half-band width 140 nm) was obtained with filter CS 7-54; the region of 300–420 nm (half-band width 75 nm) was obtained with filters CS 7-54 and CS 0-54 in combination. Light intensities incident on the samples were measured with a thermopile (Eppley) and found to correspond to 41.8 and 35.4 m watt  $\text{cm}^{-2}$ , respectively, for the two wavelength ranges employed.

The rate of weight loss of the films during irradiation was measured using the Cahn-RG electrobalance according to the technique described previously.<sup>6</sup>

Volatile degradation products formed on irradiation were collected by performing the experiments in sealed quartz cells. After irradiation, the products were removed via a break seal and analyzed by mass spectrometry and gas-liquid chromatography. The Atlas CH4 was used for the mass-spectrometric analyses while the gas-chromatographic analyses were performed using a temperature-programmed Hewlett-Packard 5750 research instrument equipped with both flame ionization and thermal conductivity detectors. A 6 ft  $\times$   $3/16$  in. molecular sieve 5A column was employed for the determination of noncondensable products; and a 6 ft  $\times$   $3/16$  in. Porapak R column was used for the analysis of condensable products.

A Beckman IR8 double-beam grating spectrometer was used to record the transmission infrared spectra of the irradiated films. The film strips were

mounted between sodium chloride plates, with one drop of tetrachloroethylene on each side of the film to prevent the recording of troublesome interference bands. The concentration of free carboxylic acid endgroups ( $-\text{COOH}$ ) in the films was determined from the optical density of the absorption band at  $3290\text{ cm}^{-1}$  assigned to the  $\text{O}-\text{H}$  vibration of the  $-\text{COOH}$  group.<sup>1</sup> A molar extinction coefficient of  $\epsilon = 150 \pm 15$  was used for these calculations based on comparison of the O.D. of the  $3290\text{-cm}^{-1}$  band and the acid equivalent of several irradiated PET samples. These acid equivalents were determined by the nonaqueous titration of a solution of PET in phenol-chloroform with standard potassium hydroxide solution in benzyl alcohol, in a similar manner to that employed by Lingen.<sup>7</sup> The value for  $\epsilon$  obtained by this technique is in excellent agreement with that reported by Ward<sup>8</sup> of  $\epsilon = 150 \pm 18$ .

## RESULTS

The results of both the mass-spectrometric analyses and gas-chromatographic analyses indicated  $\text{CO}$  and  $\text{CO}_2$  to be the main volatile products, accounting for over 90% of the total volatiles. The other products detected, although present in only small amounts, included hydrogen, methane, water, ethylene, ethane, methanol, butane, acetic acid, formaldehyde, benzene, and toluene. For example, the principal volatile products detected as a result of irradiation with 225–420 nm light under vacuum are summarized in Table I. The other products mentioned above but not listed in Table I were found only in trace amounts ( $<1$  mole-%).

The rates of formation of  $\text{CO}$ ,  $\text{CO}_2$ , and  $-\text{COOH}$  endgroups as a function of irradiation time are illustrated in Figures 1 to 4 for the variety of experimental conditions employed. In each case the initial rates were estimated from the slopes shown in the appropriate figures. From these results, together with light intensities at the front surface of the films, the known spectral distribution of the lamp, and the optical densities for PET as a

TABLE I  
Volatile Products (Mole-%) Detected on Exposure to 225–420 nm Light Under Vacuum<sup>a</sup>

Product	Product concn., mole-%				
	6 hr <sup>b</sup>	12 hr	24 hr	36 hr	48 hr
$\text{CO}$	62.3	60.1	58.5	55.7	56.6
$\text{CO}_2$	30.4	31.8	33.3	35.4	34.4
$\text{H}_2$	3.0	4.0	3.4	3.0	2.9
$\text{CH}_4$	2.2	2.9	3.0	3.0	4.6
$\text{C}_2\text{H}_6$	2.1	1.2	1.8	2.8	1.3
Total moles formed, <sup>c</sup> moles/l.	0.12	0.20	0.30	0.38	0.39

<sup>a</sup> Irradiations performed on 14-mg film samples  $21\ \mu$  thick and 1.398 density.

<sup>b</sup> Irradiation time.

<sup>c</sup> Calculated on the basis of 1 liter of film.

function of wavelength, calculations were made of the quantum yields for the products measured. The optical densities of the film in the 310–420 nm range as measured by UV spectroscopy were corrected for light scattering at the surface and in the interior of the film according to the procedure outlined previously.<sup>2</sup> The quantum yields obtained from these calculations are summarized in Table II.

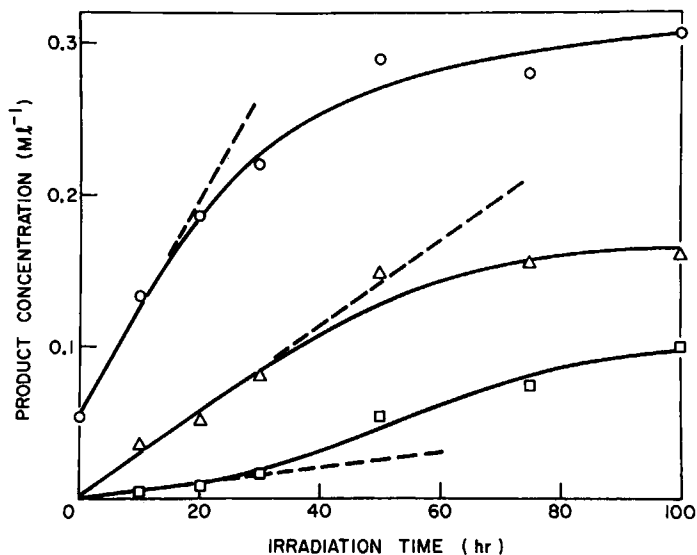


Fig. 1. Product formation on exposure of PET to 300–420 nm light under vacuum: (O) —COOH endgroups; ( $\Delta$ ) CO; ( $\square$ )  $\text{CO}_2$ .

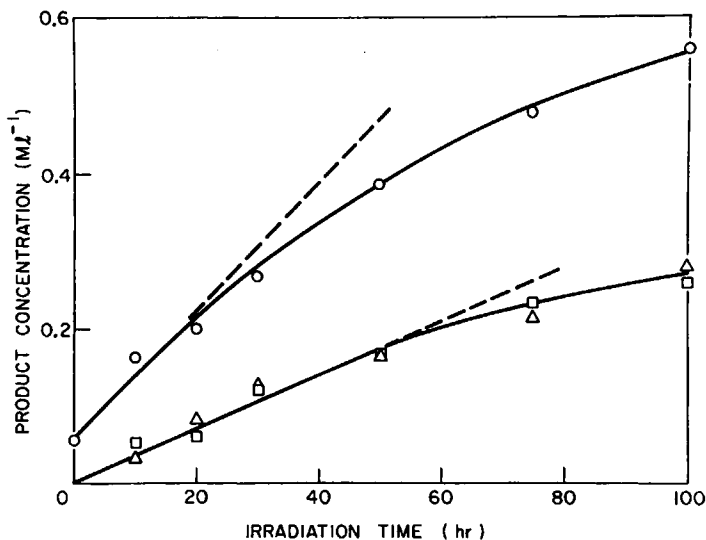


Fig. 2. Product formation on exposure of PET to 300–420 nm light in air: (O) —COOH endgroups; ( $\Delta$ ) CO; ( $\square$ )  $\text{CO}_2$ .

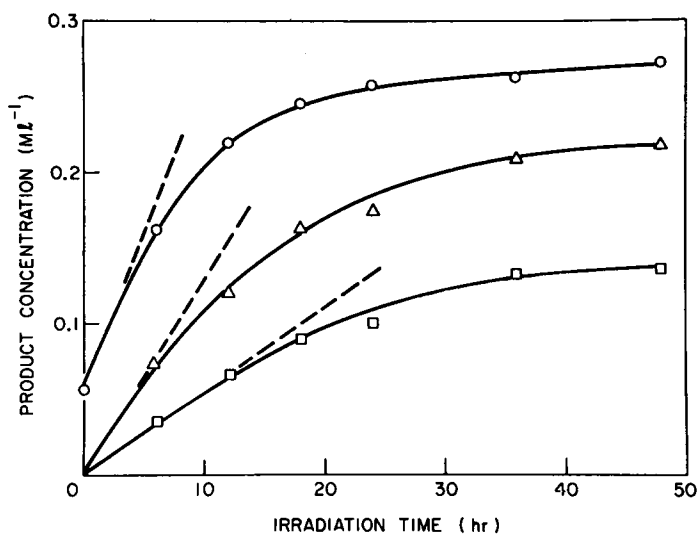


Fig. 3. Product formation on exposure of PET to 225–420 nm light under vacuum: (O) —COOH endgroups; ( $\Delta$ ) CO; ( $\square$ ) CO<sub>2</sub>.

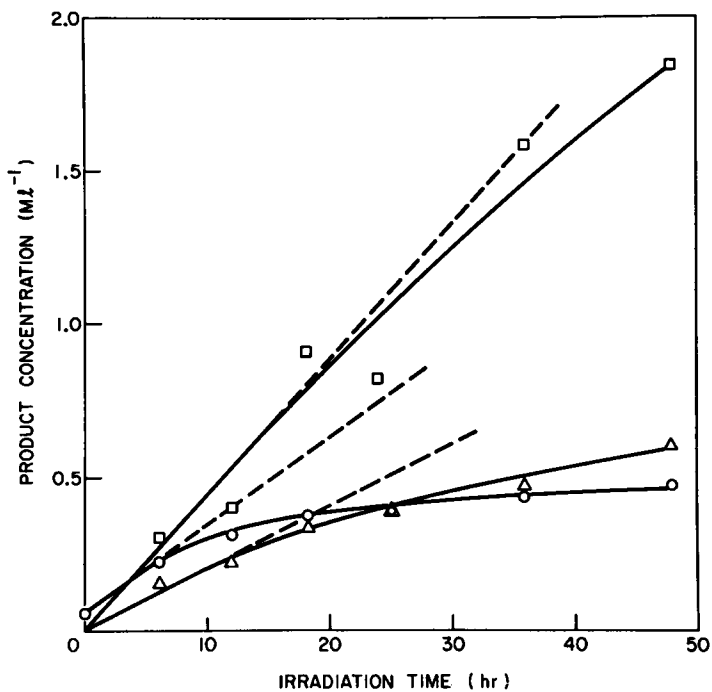


Fig. 4. Product formation on exposure of PET to 225–420 nm light in air: (O) —COOH endgroups; ( $\Delta$ ) CO; ( $\square$ ) CO<sub>2</sub>.

The changes in weight of the polymer film with irradiation time are compared with the corresponding total weight production for CO and CO<sub>2</sub> in Figures 5 and 6 for the filter ranges of 300–420 nm and 225–420 nm, respectively.

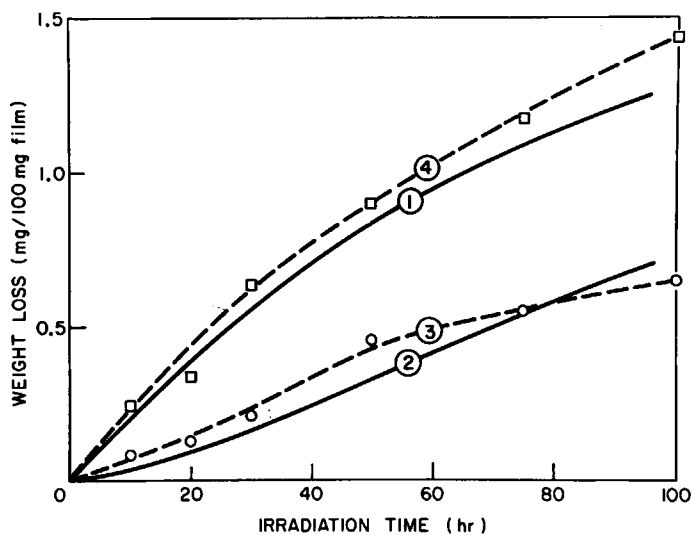


Fig. 5. Changes in weight during irradiation with 300–420 nm light: (—) observed total weight loss, (1) under vacuum, (2) in air; (---) calculated weight loss due to CO + CO<sub>2</sub> from GC analysis, (3) under vacuum, (4) in air.

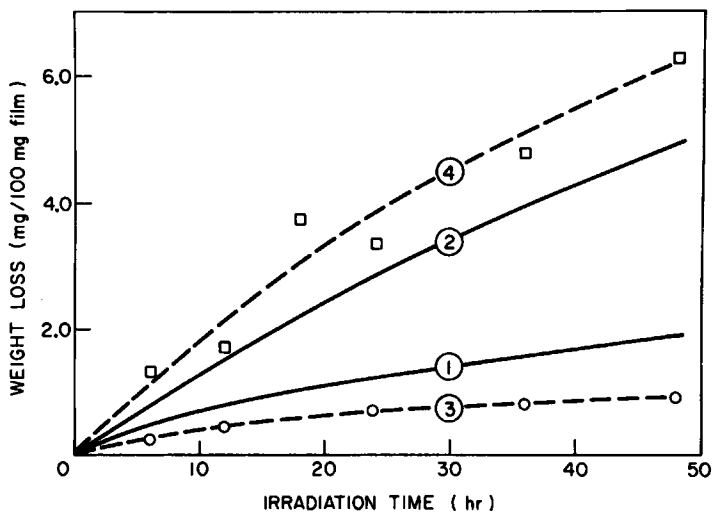


Fig. 6. Changes in weight during irradiation with 225–420 nm light: (—) observed total weight loss, (1) under vacuum, (2) in air; (---) calculated weight loss due to CO + CO<sub>2</sub> from GC analysis, (3) under vacuum, (4) in air.

TABLE II  
Initial Quantum Yields ( $\times 10^4$ )

Wavelength, nm	Environment	CO	CO <sub>2</sub>	—COOH
300–420	vacuum	6.1	1.1	17.2
225–420	vacuum	8.5	3.6	13.9
300–420	air	8.7	8.7	18.3
225–420	air	12.8	28.3	20.3

## DISCUSSION

The relative product distribution of the main products of photochemical degradation appear to be dependent, to some extent, on whether oxygen is present in the system and, to a lesser extent, on the wavelength of irradiation. Thus, it appears to be feasible to distinguish between direct photolysis and photo-oxidation and between initial primary reactions and subsequent secondary reactions.

### Vacuum Photolysis

It is of interest first to consider the results obtained on vacuum photolysis (Figs. 1 and 3). The initial quantum yields for CO, CO<sub>2</sub>, and —COOH were essentially the same for the two wavelength ranges used for irradiation. The values for CO and —COOH are, however, much higher than those for CO<sub>2</sub>. From these results it was concluded that the primary initial photolytic reactions involve the formation of CO and —COOH endgroups, while

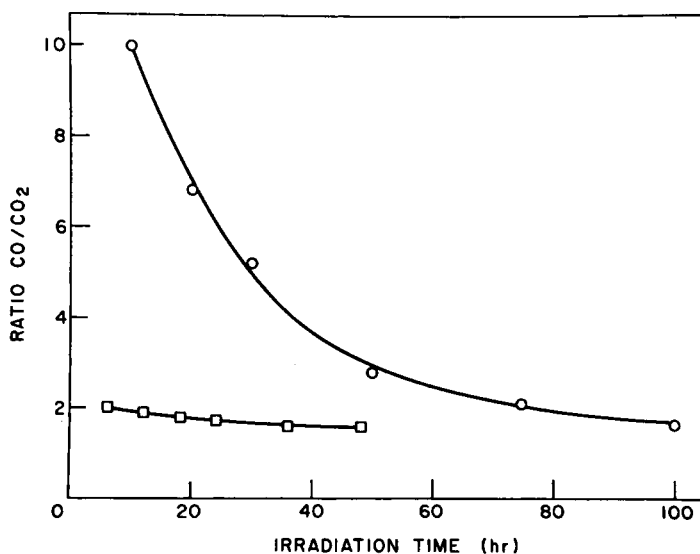
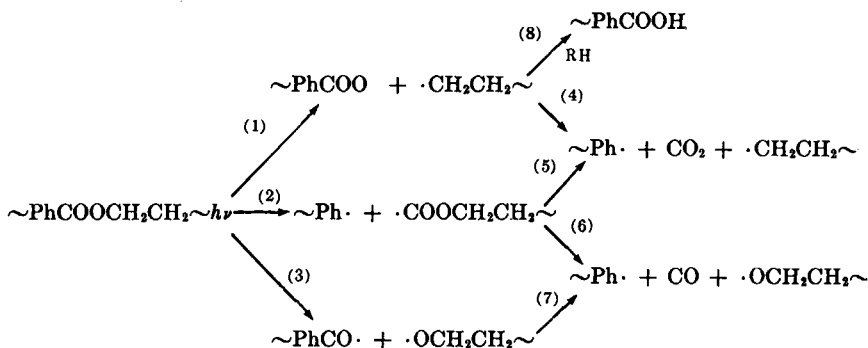


Fig. 7. Ratio of the concentration of CO and CO<sub>2</sub> formed under vacuum on exposure of PET to: (O) 300–420 nm light; (□) 225–420 nm light.

the formation of  $\text{CO}_2$  is only of importance later in the decomposition. This conclusion is consistent with the observation of an induction period in the  $\text{CO}_2$  production (Fig. 1) and also with the changes in the ratio of CO to  $\text{CO}_2$  formation during irradiation (Fig. 7).

Quantum yields for the photolysis of PET have been reported by Marcotte<sup>9</sup> who obtained values of  $6 \times 10^{-4}$ ,  $2 \times 10^{-4}$ ,  $5.5 \times 10^{-4}$ , and  $1.5 \times 10^{-4}$  for the production of CO,  $\text{CO}_2$ , crosslinking and trapped radical formation, respectively, when 313-nm light was employed. Using 253.7-nm light, he found the quantum yields ( $\times 10^4$ ) for CO and  $\text{CO}_2$  formation to be 6–9 and 2–3, respectively, in general agreement with the results shown in Table II. However, it should be noted that Marcotte<sup>9</sup> obtained a quantum yield for chain fractures of  $16 \times 10^{-4}$  and was unable to account for it in terms of CO and  $\text{CO}_2$  production; he did not speculate on the reason for the discrepancy. Examination of our data, however, indicates that the additional fracture reaction which results in the formation of  $-\text{COOH}$  end-groups should be considered. By making allowance for such a reaction, it is possible to decide on the relative importance of the possible reaction mechanisms responsible for the photochemical decomposition of PET.

From the data obtained in this study, we propose reaction mechanisms to account for our main findings, namely that  $-\text{COOH}$  and CO are the main products of photolysis, with  $\text{CO}_2$  being of secondary importance. The following primary photolytic chain scissions may be postulated in that they give the required products:



Although accurate bond dissociation energies are not known for the relevant bonds in PET, estimates can be made from the thermochemical data for the model compound ethyl benzoate. Based on the standard heats of formation of ethyl benzoate and the related free radicals as shown in Table III, the bond dissociation energies related to the primary scission reactions (1), (2), and (3) have been estimated to be 84, 102, and 88 kcal/mole, respectively.

On energetic grounds, reaction (2) appears to be unlikely in comparison to the alternate reaction (3) for the formation of CO. It thus seems likely that for the production of CO, the favored reaction sequence is (3) + (7).





containing a  $\gamma$ -hydrogen atom decompose photochemically by an intramolecular rearrangement into an olefin and the corresponding acid. This Norrish type II photoelimination reaction has also been verified for the photolysis of undiluted di-*n*-butyl terephthalate which gave high yields of 1-butene and —COOH endgroups at comparable rates.<sup>16</sup> Although molecular motion is relatively restricted in the solid phase, the gauche isomer, as observed in the amorphous region of PET,<sup>17,18</sup> is conducive to the formation of the required six-centered transition state.

Examination of the rate of formation of CO<sub>2</sub> under vacuum with 300–420 nm irradiation (Fig. 1) indicates that it is produced initially in only small amounts during an apparent induction period before the rate of its production increases. Thus, it may be assumed that the CO<sub>2</sub> is initially produced by a process such as reaction (1) + (4). However, at a later stage in the photolysis, it is probably being produced, in addition, from an intermediate whose concentration has built up with time as irradiation proceeds. This would then account for the apparent induction period observed and the subsequent change in the CO/CO<sub>2</sub> ratio. This change in ratio of CO to CO<sub>2</sub> during vacuum photolysis has also been observed by Marcotte<sup>9</sup> who obtained a limiting value of 1.5, in very good agreement with the data presented in Figure 7.

The reason for the slightly higher initial quantum yield for CO<sub>2</sub> obtained with 225–420 nm radiation in comparison with that obtained with 300–420 nm radiation has not been resolved. It appears, however, that it may be attributed to the improved efficiency of the (1) + (4) reactions at shorter wavelengths.

While analysis of the volatile degradation products indicates CO and CO<sub>2</sub> to be the main products, accounting for over 90% of the total volatiles on a mole basis, it can be seen from Figures 5 and 6 that on a weight basis they account only for approximately 55% of the total weight loss. Correcting for the other products listed in Table I raises this value to approximately 58%, which still leaves 40% to be accounted for. However, in view of the presence in the films of low molecular weight oligomers, their contribution to the weight loss may be significant. It was not possible to detect their presence in the volatiles, but solids build-up by sublimation on parts of the apparatus suggests loss of oligomers from the films during irradiation.

### Photo-oxidation

These studies were performed under exactly the same conditions as the vacuum experiments, with the exception that air was present in these systems at a pressure of 1 atm at the onset of irradiations. Under the photo-oxidative conditions being employed, however, straight photolysis was still an important feature of the reaction. No major differences were observed in the composition of the volatile products when the experiments were performed in air instead of under vacuum, with the exception that the production of CO<sub>2</sub> was greatly enhanced. The results obtained with the two separate wavelength regions will be considered individually.



This monohydroxy species has been reported to be responsible for the fluorescence observed in photo-oxidized PET.<sup>24</sup> The fact that this fluorescent product is only observed under photo-oxidative conditions<sup>2</sup> appears to substantiate the above photo-oxidative mechanism involving hydroperoxide formation and photolysis.

Comparison of the total weight loss with the weight lost due to CO plus CO<sub>2</sub> (Fig. 5) indicates that the actual decrease in film weight is small in comparison to the CO and CO<sub>2</sub> evolved. This indicates that photo-oxidation is occurring in which oxygen is being consumed, giving rise to nonvolatile products within the polymer.

#### *225-420 nm Light*

The quantum yield for production of —COOH endgroups appears to be independent of the wavelength of irradiation, as well as being independent of the irradiation environment. Thus the mechanism proposed previously for their formation appears to be equally applicable under these wider wavelength conditions of irradiation. The quantum yields for the production of CO and CO<sub>2</sub>, however, are larger than those obtained with the 300-420 nm light. This increase in the rate of production of CO and CO<sub>2</sub> with the wider wavelength range may be attributed to the decomposition of secondary oxidative products within the polymer which are susceptible to the shorter wavelength light. This appears to be substantiated by the weight loss curves in Figure 6, where it is shown that the total weight loss is substantially greater than that obtained with 300-420 nm light. It appears that the partial compensation in weight loss observed with 300-420 nm light, due to the formation of oxidation products within the polymer is no longer valid. Instead, it is now apparent that these oxidation products are being decomposed by the short wavelength light with the resulting greater production of CO and CO<sub>2</sub>. It may be concluded that no major differences are involved in the primary photolytic processes with the use of the short wavelength light; it is only the formation and subsequent decomposition of secondary oxidation products that is substantially different.

### CONCLUSIONS

In summarizing the data presented in this paper, the following observations may be made regarding the mechanism of the photochemical decomposition of PET, within the context of the experimental conditions employed:

1. The main initial reactions leading to the production of —COOH endgroups appear to be independent of the wavelength and environment and occur via a Norrish type II photoelimination, reaction (10).
2. The mechanism for the production of CO also appears to be independent of environment and wavelength and consists of the primary photolytic chain scission sequence (3) + (7).

3. CO<sub>2</sub> appears to be produced mainly as a result of photo-oxidation since its formation is greatly enhanced during irradiations in the presence of air. A likely mechanism to account for this involves hydroperoxide formation, reactions (11)–(15).

4. The hydroperoxide decomposition mechanism is consistent with the probable secondary reactions involved in the formation of the fluorescent product.

5. Photo-oxidation gives rise to nonvolatile products within the polymer when long wavelength radiation is employed. These oxidation products are photochemically degraded to give additional CO and CO<sub>2</sub> when shorter wavelength irradiation conditions are employed.

NRCC No. 12314.

### References

1. M. Day and D. M. Wiles, *J. Appl. Polym. Sci.*, **16**, 175 (1972).
2. M. Day and D. M. Wiles, *J. Appl. Polym. Sci.*, **16**, 191 (1972).
3. J. H. Dumbleton and B. B. Bowles, *J. Polym. Sci. A<sub>2</sub>*, **4**, 951 (1966).
4. D. A. S. Ravens and I. M. Ward, *Trans. Faraday Soc.*, **57**, 150 (1961).
5. L. H. Peebles, M. W. Huffman, and C. T. Ablett, *J. Polym. Sci. A<sub>1</sub>*, **7**, 479 (1969).
6. D. J. Carlsson and D. M. Wiles, *Macromolecules*, **2**, 587 (1969).
7. R. L. M. van Lingen, *Z. Anal. Chem.*, **247**, 232 (1969).
8. I. M. Ward, *Trans. Faraday Soc.*, **53**, 1406 (1957).
9. F. B. Marcotte, D. Campbell, J. A. Cleaveland, and D. T. Turner, *J. Polym. Sci. A<sub>1</sub>*, **5**, 481 (1967).
10. J. A. Kerr, *Chem. Rev.*, **66**, 465 (1966).
11. P. Gray, *Advan. Chem. Ser.*, **75**, 282 (1968).
12. C. A. Barson and J. C. Bevington, *Tetrahedron*, **4**, 147 (1958).
13. T. G. Traylor, A. Sieber, H. Kiefer, and N. Clinton, *Intra Sci. Chem. Rep.*, **3**, 289 (1969).
14. P. Ausloos, *Can. J. Chem.*, **36**, 383 (1958).
15. J. A. Barltrop and J. D. Coyle, *J. Chem. Soc. (B)*, 251 (1971).
16. M. Day and D. M. Wiles, *Can. J. Chem.*, **49**, 2916 (1971).
17. T. R. Manley and D. A. Williams, *J. Polym. Sci. C*, **22**, 1009, (1969).
18. N. A. Slovokhotova, G. K. Sadovskaya, and V. A. Kargin, *J. Polym. Sci.*, **58**, 1293 (1962).
19. O. Cicchetti, *Advan. Polym. Sci.*, **7**, 70 (1970).
20. D. J. Carlsson and D. M. Wiles, *Macromolecules*, **2**, 597 (1969).
21. E. Jaworska and W. Zielinski, *Polimery*, **14**, 284 (1969).
22. G. Valk, M. L. Kehren, and I. Daamen, *Angew. Macromol. Chem.*, **13**, 97 (1970).
23. L. H. Buxbaum, *Angew. Chem. (Int. Ed.)*, **7**, 182 (1968).
24. J. G. Pacifici and J. M. Straley, *Polymer Letters*, **7**, 7 (1969).

Received June 30, 1971

Revised September 7, 1971